



Cite this: *Chem. Commun.*, 2016, 52, 12893

Received 24th August 2016,  
Accepted 6th October 2016

DOI: 10.1039/c6cc06943f

www.rsc.org/chemcomm

# A drastic change in the superhydrophilic crystal porosities of metallosupramolecular structures via a slight change in pH†

Sireenart Surinwong, Nobuto Yoshinari, Tatsuhiro Kojima and Takumi Konno\*

**A unique pH-controlled synthesis of two metallosupramolecular structures from  $\text{Co}_2^{\text{III}}\text{Au}_3^{\text{I}}$  complex anions and  $\text{Zn}^{\text{II}}$  cations is reported. A dense coordination polymer (porosity ~13%) was formed at a pH of 5.0, whereas a porous ionic framework (porosity ~61%) that selectively adsorbs  $\text{CO}_2$  and  $\text{H}_2\text{O}$  was created when the pH was adjusted to 5.5.**

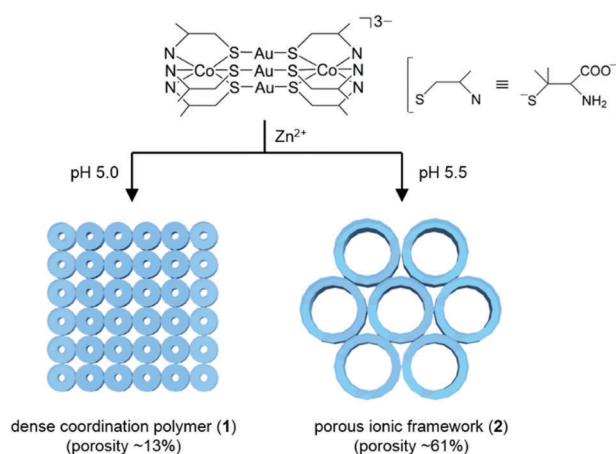
The preparation of porous crystalline materials such as metal-organic frameworks (MOFs), coordination polymers (CPs), and porous ionic frameworks has received continuous attention not only because of these materials' fascinating structures but also because of their unique properties for gas storage and separation, chemical sensing, catalysis, *etc.*<sup>1–3</sup> However, controlling the crystal porosities of this class of materials is frequently very difficult because of the effects of various synthesis parameters, including pH, solvent, and concentration, on the interactions between the metal ions and ligands.<sup>4</sup> Therefore, the systematic synthesis of porous crystalline materials with the desired porosity by controlling these external factors remains an important research topic.

pH is one of the external stimuli that most strongly influence the construction of porous crystalline materials.<sup>5</sup> This influence stems from the effect of changes in pH on the protonation level, which drastically changes the coordination modes and conformations of ligands, the geometry of metal centres, and the intermolecular hydrogen bonding interactions.<sup>5,6</sup> Previous reports on the pH effect on the production of MOFs revealed that a higher pH tends to give frameworks with greater dimensionality compared to those formed at a lower pH.<sup>6</sup> However, a systematic approach to controlling crystal porosities by alteration of pH has thus far been much less explored.

Herein, we report a unique metallosupramolecular system that exhibits a drastic increase in crystal porosity with an increase

in the pH of reaction solutions. This system involves a dense coordination polymer,  $[\text{Zn}(\text{H}_2\text{O})_4\{\text{Co}_2\text{Au}_3(\text{D-Hpen-N,S})(\text{D-pen-N,S})_5\}]$  (**1**; porosity ~13%, D-H<sub>2</sub>pen = D-penicillamine), and a highly porous ionic compound,  $\text{Na}_9[\text{Zn}(\text{OAc})_2\{\text{Co}_2\text{Au}_3(\text{D-pen-N,S})_6\}_2][\text{Co}_2\text{Au}_3(\text{D-pen-N,S})_6]$  (**2**; porosity ~61%), both of which are independently produced from rod-shaped  $\text{Co}_2^{\text{III}}\text{Au}_3^{\text{I}}$  pentanuclear complex-anions  $[\text{Co}_2\text{Au}_3(\text{D-pen-N,S})_6]^{3-}$  and  $\text{Zn}^{2+}$  cations at slightly different solution pH levels (5.0 vs. 5.5) (Scheme 1). To the best of our knowledge, such a drastic increase in crystal porosity from a dense coordination polymer to a porous ionic compound has not been previously reported.

Solutions of  $\text{Na}_3[\text{Co}_2\text{Au}_3(\text{D-pen-N,S})_6]^{3-}$  and  $\text{Zn}(\text{OAc})_2$  in a sodium acetate buffer solution at pH 4.5 ( $\text{HOAc}/\text{NaOAc} = 1:1$ ) were mixed together, yielding insoluble purple crystals with a square block shape (**1**).† The crystallization of **1** was complete within a day, with a yield of 58%. The diffuse reflection spectrum of **1** and the solid-state circular dichroism (CD) spectrum are similar to those of  $\text{Na}_3[\text{Co}_2\text{Au}_3(\text{D-pen-N,S})_6]^{3-}$ , indicating that the S-bridged pentanuclear structure in  $[\text{Co}_2\text{Au}_3(\text{D-pen-N,S})_6]^{3-}$  is



**Scheme 1** Synthetic routes and schematics of two different metallosupramolecular structures (**1** and **2**) constructed from  $[\text{Co}_2\text{Au}_3(\text{D-pen-N,S})_6]^{3-}$  anions and  $\text{Zn}^{2+}$  cations at various pH values.

Department of Chemistry, Graduate School of Science, Osaka University, Toyonaka, Osaka 560-0043, Japan. E-mail: konno@chem.sci.osaka-u.ac.jp

† Electronic supplementary information (ESI) available: Details of syntheses together with spectroscopic data, adsorption data, PXRD results, and single-crystal X-ray diffraction data. CCDC 1500233 and 1500234. For ESI and crystallographic data in CIF or other electronic format see DOI: 10.1039/c6cc06943f



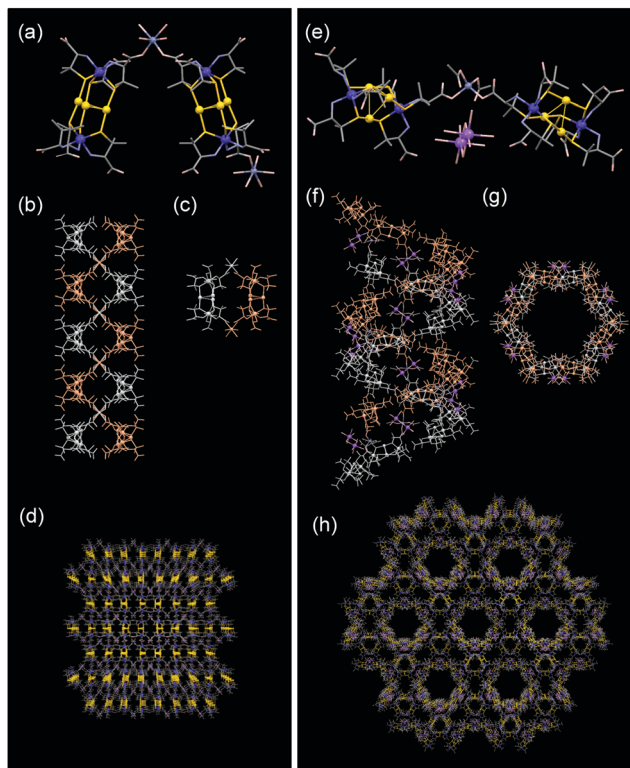


**Fig. 1** Perspective views of (a) the expanded asymmetric unit, (b) side and (c) top views of the right-handed 2-fold double helix structure (orange and white), and (d) a 3D dense structure with 1D coordination polymers in **1**. Perspective views of (e) the expanded asymmetric unit, (f) side and (g) top views of the right-handed 6-fold double-helix structure (orange and white), and (h) a 1D channel structure in **2**. Colour codes: Zn, dark grey; Na, red purple; Co, deep blue; Au, gold; S, yellow; O, pink; N, blue; C, grey. Dashed lines indicate hydrogen bonds.

retained in **1** (Fig. S1a and S2a).<sup>†</sup> The IR spectrum of **1** shows an intense C=O stretching band at  $1609\text{ cm}^{-1}$  with a shoulder at  $1717\text{ cm}^{-1}$ . The former and the latter correspond to deprotonated  $\text{COO}^-$  and protonated  $\text{COOH}$  groups, indicative of the partial protonation of carboxylate groups in **1** (Fig. S3).<sup>†</sup> X-ray fluorescence analysis confirmed the existence of Zn atoms, in addition to the Co and Au. Combining these results with the elemental analysis data, we predicted that **1** is a 1:1 adduct of  $\text{Zn}^{2+}$  and  $[\text{Co}_2\text{Au}_3(\text{D-pen-N,S})(\text{D-pen-N,S})_5]^{2-}$ , in which one of the six D-pen carboxyl groups is protonated.

The structure of **1** was determined by single-crystal X-ray diffraction analysis. In addition to the water molecules of crystallization, **1** contains *cis*-configurational  $[\text{Zn}(\text{H}_2\text{O})_4]^{2+}$  cations directly bound to  $[\text{Co}_2\text{Au}_3(\text{D-pen-N,S})(\text{D-pen-N,S})_5]^{2-}$  anions (Fig. 1a). In **1**,  $[\text{Co}_2\text{Au}_3(\text{D-pen-N,S})(\text{D-pen-N,S})_5]^{2-}$  anions are alternately connected by the  $[\text{Zn}(\text{H}_2\text{O})_4]^{2+}$  cations through coordination bonds (av.  $\text{Zn}-\text{OOC} = 2.02\text{ \AA}$ ), forming a 2-fold helix along the crystallographic *a* axis (Fig. 1b and c). Additionally, the two helices are intertwined and connected to each other through  $\text{OH}_2 \cdots \text{OOC}$  hydrogen bonds (av.  $\text{O} \cdots \text{O} = 2.72\text{ \AA}$ ), forming a tight right-handed double-helix structure (Fig. S4 and S5).<sup>†</sup> The double helices are connected to each other through  $\text{COOH} \cdots \text{OOC}$  intermolecular hydrogen-bonding interactions (av.  $\text{O} \cdots \text{O} = 2.84\text{ \AA}$ ) to

form a 2D sheet-like structure (Fig. S6).<sup>†</sup> Finally, the 2D sheets are stacked through  $\text{NH}_2 \cdots \text{OOC}$  hydrogen bonds (av.  $\text{N} \cdots \text{O} = 2.98\text{ \AA}$ ), completing a 3D dense structure (Fig. 1d). The estimated solvent accessible volume of **1** was  $\sim 13\%$  on the basis of our calculations using the PLATON program.<sup>9</sup>

A similar treatment of  $\text{Na}_3[\text{Co}_2\text{Au}_3(\text{D-pen-N,S})_6]$  and  $\text{Zn}(\text{OAc})_2$  in a sodium acetate buffer solution at pH 5.0 ( $\text{HOAc}/\text{NaOAc} = 1:2$ ) also yielded only insoluble purple square block crystals of **1**. New water-soluble purple hexagonal block crystals (**2**) were obtained when the pH of the buffer solution was increased to 5.5 ( $\text{HOAc}/\text{NaOAc} = 1:6$ ).<sup>†</sup> The diffuse reflection and solid-state CD spectra of **2** are essentially the same as those of **1** (Fig. S1b and S2b).<sup>†</sup> However, the IR spectrum displays a C=O stretching absorption only at  $1611\text{ cm}^{-1}$  (Fig. S3), indicating that all carboxyl groups in **2** are deprotonated.<sup>†</sup> The X-ray fluorescence and elemental analysis results were in good agreement with a 1:3 adduct of  $\text{Zn}^{2+}$  and  $[\text{Co}_2\text{Au}_3(\text{D-pen-N,S})_6]^{3-}$ . In addition,  $^{23}\text{Na}$  and  $^1\text{H}$  NMR spectra revealed the presence of  $\text{Na}^+$  and  $\text{OAc}^-$  ions, respectively (Fig. S7 and S8).<sup>†</sup> Single-crystal X-ray analysis revealed that **2** consists of tetrahedral  $\{\text{Zn}(\text{OAc})_2\}$  units,  $[\text{Co}_2\text{Au}_3(\text{D-pen-N,S})_6]^{3-}$  anions, in addition to aqua  $\text{Na}^+$  cations and water molecules of crystallization (Fig. 1e). In **2**,  $[\text{Co}_2\text{Au}_3(\text{D-pen-N,S})_6]^{3-}$  anions are hydrogen bonded (av.  $\text{N} \cdots \text{O} = 2.93\text{ \AA}$ ) to each other to construct a six-fold helix with right handedness along the *c* axis. The two helices are bridged by the  $\{\text{Zn}(\text{OAc})_2\}$  moieties (av.  $\text{Zn}-\text{O}_{\text{OAc}} = 1.96\text{ \AA}$ ) through coordination bonds (av.  $\text{Zn}-\text{O}_{\text{pen}} = 1.97\text{ \AA}$ ), resulting in a tubular double helix structure with a large 1D pore with a diameter of *ca.*  $20\text{ \AA}$  (Fig. 1f and g). The double helices are further connected by other  $[\text{Co}_2\text{Au}_3(\text{D-pen-N,S})_6]^{3-}$  anions *via*  $\text{NH}_2 \cdots \text{OOC}$  hydrogen bonds (av.  $\text{N} \cdots \text{O} = 2.91\text{ \AA}$ ), completing a 3D framework that possesses 1D pore channels (Fig. 1h and Fig. S9).<sup>†</sup> The channels accommodate water molecules and  $\text{Na}^+$  ions that are severely disordered. The estimated solvent accessible volume of **2** was  $\sim 61\%$ . This 1D channel structure is supported by aqua  $\text{Na}^+$  cations, each of which forms  $\text{Na}-\text{OH}_2 \cdots \text{OOC}$  hydrogen bonds (av.  $\text{O} \cdots \text{O} = 2.83\text{ \AA}$ ) between two  $[\text{Co}_2\text{Au}_3(\text{D-pen-N,S})_6]^{3-}$  anions and one  $\{\text{Zn}(\text{OAc})_2\}$  unit in the double helix.

The spatial arrangement of  $[\text{Co}_2\text{Au}_3(\text{D-pen-N,S})_6]^{3-}$  anions in **2** is reminiscent of that in the previously reported porous ionic crystal  $[\text{Co}(\text{H}_2\text{O})_4][\text{Co}(\text{H}_2\text{O})_6][\text{Co}_2\text{Au}_3(\text{D-pen-N,S})_6]_2$  (**3**).<sup>10</sup> The substitution of linking *trans*- $[\text{Co}(\text{H}_2\text{O})_4]^{2+}$  units and free  $[\text{Co}(\text{H}_2\text{O})_6]^{2+}$  ions in **3** by  $\{\text{Zn}(\text{OAc})_2\}$  units and  $[\text{Na}_2(\text{H}_2\text{O})_{10}]^{2+}$  ions in **2** is the only substantial structural difference between **2** and **3**. However, the stabilities of **2** and **3** are quite different; a powder X-ray diffraction study demonstrated that **2** retains its crystallinity after being heated at  $120\text{ }^\circ\text{C}$  for 12 h, whereas **3** collapses immediately even at room temperature (Fig. S10 and S11).<sup>†</sup> As previously mentioned, multiple hydrogen bonds exist between acetate groups from  $\{\text{Zn}(\text{OAc})_2\}$  and aqua ligands in  $[\text{Na}_2(\text{H}_2\text{O})_{10}]^{2+}$  units in **2** (Fig. S12).<sup>†</sup> By contrast, no direct hydrogen-bonding interactions were observed between *trans*- $[\text{Co}(\text{H}_2\text{O})_4]^{2+}$  units and free  $[\text{Co}(\text{H}_2\text{O})_6]^{2+}$  ions in **3**, which is most likely the reason for the substantial difference in stability between **2** and **3**.

The protonation and deprotonation of the carboxylate group at different pH values and in the presence/absence of an excess



of  $\text{Na}^+$  and  $\text{OAc}^-$  ions in reaction solutions are potential causes of the drastic change in crystal porosity between **1** and **2**. In **1**, the protonated D-pen carboxyl groups form strong intermolecular  $\text{COOH} \cdots \text{OOC}$  hydrogen bonds, which bring neighbouring helices much closer. Consequently, a dense structure with low porosity ( $\sim 13\%$ ) was reasonably constructed. In this case, the presence of both the protonated and the deprotonated carboxylate groups in each complex anion in the pH range from 4.0 to 5.0 is reasonable.<sup>11</sup> By contrast, a slight but higher pH value of 5.5 leads to a fully deprotonated form of D-pen in **2**. Unlike in **1**,  $\text{Na}^+$  and  $\text{OAc}^-$  ions from the employed NaOAc buffer solution were incorporated into **2**. Both  $\text{Na}^+$  and  $\text{OAc}^-$  ions appear to be associated with the template-directed synthesis of **2**, i.e. these ions form strong intermolecular hydrogen bonds to stabilize the 1D channel structure with substantially increased porosity. Presumably, the formation of **2** was accomplished with the aid of the stabilizing effect due to a large amount of  $\text{Na}^+$  and  $\text{OAc}^-$  ions in a basic acetate buffer solution. However, we observed that **1** was also selectively produced using controlled experiments in the pH range from 4.0 to 5.0 when the reaction solutions contained the same amounts of  $\text{Na}^+$  and  $\text{OAc}^-$  ions as those of **2** (Fig. S13).<sup>†</sup> This is because a large part of  $\text{OAc}^-$  ions exist in a protonated form in this pH range to prevent the coordination to a  $\text{Zn}^{2+}$  centre. Thus, we concluded that pH is the dominant factor controlling the crystal porosities in the present metallosupramolecular system, changing the protonation/deprotonation states of the carboxylate groups.

The gas adsorption properties of **1** and **2** were investigated. As shown in Fig. S14, the  $\text{CO}_2$  adsorption isotherm for **1** at 195 K displayed a type-I physical sorption isotherm,<sup>12</sup> showing a gradual increase to  $8.7 \text{ cm}^3 \text{ g}^{-1}$  at  $P/P_0 = 0.99$ , with a low calculated BET surface area of  $16 \text{ m}^2 \text{ g}^{-1}$ .<sup>†</sup> A similar  $\text{CO}_2$  adsorption isotherm was observed for **2**; however, the adsorption amounts increased to a saturation value of  $29.3 \text{ cm}^3 \text{ g}^{-1}$  at  $P/P_0 = 0.99$  because of its higher porosity. The BET surface area calculated from the  $\text{CO}_2$  adsorption isotherm was also substantially greater:  $66 \text{ m}^2 \text{ g}^{-1}$ . By contrast, the adsorption capacities of  $\text{N}_2$  gas for both compounds (Fig. S15 and S16) were very poor at 77 K ( $< 5.0 \text{ cm}^3 \text{ g}^{-1}$ ).<sup>†</sup> The adsorption properties toward small vapour molecules were also investigated. Although the degree of water molecule adsorption for **1** was quite small ( $5 \text{ mol mol}^{-1}$  at  $P/P_0 = 0.90$ ), **2** exhibited an impressively high adsorption of  $134 \text{ mol mol}^{-1}$  ( $584 \text{ cm}^3 \text{ g}^{-1}$ ) at  $P/P_0 = 0.90$  (Fig. 2). This adsorption value is comparable to those for MOFs with excellent water adsorption ability.<sup>¶13,14</sup> Notably, the ionic compound **2** possesses a substantial advantage over the MOFs that are commonly insoluble in solution because it can be regenerated *via* a dissolution–crystallization process. In an adsorption–desorption cycle, a large hysteresis loop was observed for **2**, which is typical for nanoporous materials with large pores.<sup>14</sup> Remarkably, not only **1** but also **2** exhibited no adsorption ability toward EtOH and acetone molecules (Fig. S17 and S18), reflecting the superhydrophilic character of their porous structures surrounded by numerous hydrophilic groups.<sup>†15</sup> Previously, similar superhydrophilic behaviour was observed for **3**. However, the adsorption capacity of **2** is much

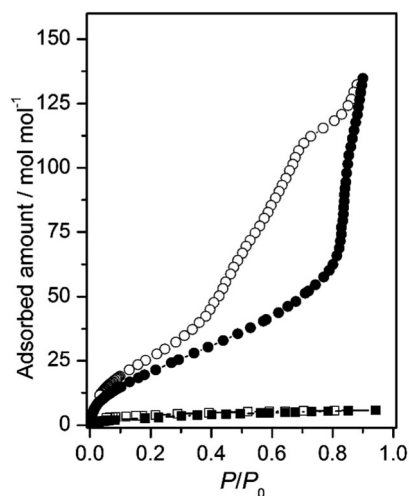


Fig. 2 Comparison of  $\text{H}_2\text{O}$  adsorption (solid symbols) and desorption (open symbols) isotherms at 298 K for **1** (—■—) and **2** (—●—).

greater than that of **3** ( $33 \text{ mol mol}^{-1}$  at  $P/P_0 = 0.90$ ), which is ascribed to the very rigid porous framework in **2**.

In summary, we demonstrated that two metallosupramolecular compounds (**1** and **2**) of remarkably different porosities ( $\sim 13\%$  and  $\sim 61\%$ , respectively) can be independently created from  $[\text{Co}_2\text{Au}_3(\text{D-pen-N,S})_6]^{3-}$  anions and  $\text{Zn}^{2+}$  cations with only a slight change in solution pH (5.0 vs. 5.5). Such a drastic change in crystal porosities by a slight change in pH has not been previously reported for crystalline coordination compounds. The formation of stable, superhydrophilic opening channels in **2**, which are applicable for the selective inclusion of hydrophilic small molecules, is noteworthy. This study should serve as a guide for further development of the synthesis of reproducible, functional porous materials consisting of cationic and anionic species.

This work was supported by CREST, JST and JSPS KAKENHI Grant Number 15K21127 and 16K13609. The synchrotron radiation experiments were performed at the BL02B1 and BL02B2 beamlines of SPring-8 with the approval of the Japan Synchrotron Radiation Research Institute (JASRI) (Proposal No. 2015B1001, 2015B1237, 2016A1073) and at the 2D beamline in the Pohang Accelerator Laboratory supported by POSTECH.

## Notes and references

<sup>†</sup> Similar reactions in a sodium acetate buffer solution at pH 6.0 and 6.5 also gave **2**.

<sup>§</sup> When **1** was dissolved in a sodium acetate buffer solution of pH 5.5, **2** was selectively crystallized after several days. The reverse conversion from **2** into **1** also occurred when a sodium acetate buffer solution of pH 5.0 was employed.<sup>†</sup>

<sup>¶</sup> Although the water adsorption amount of **2** is lower than the reported record for MOFs (PZOF-2;  $850 \text{ cm}^3 \text{ g}^{-1}$ ),<sup>13</sup> this is the highest value for a porous ionic framework.

- (a) S. Kitagawa, R. Kitaura and S. Noro, *Angew. Chem., Int. Ed.*, 2004, **43**, 2334; (b) J. R. Li, R. J. Kuppler and H. C. Zhou, *Chem. Soc. Rev.*, 2009, **38**, 1477; (c) R. Eguchi, S. Uchida and N. Mizuno, *Angew. Chem., Int. Ed.*, 2012, **51**, 1635; (d) R. Eguchi, S. Uchida and N. Mizuno, *J. Phys. Chem. C*, 2012, **116**, 16105; (e) S. Uchida, R. Kawahara, Y. Ogasawara and N. Mizuno, *Dalton Trans.*, 2013, **42**, 16209; (f) H. Furukawa, K. E. Cordova, M. O'Keeffe and O. M. Yaghi, *Science*, 2013, **341**, 974; (g) Y. Mito-oka, Y. Sawada,



- T. Masumori, S. Horike, H. Kitagawa and S. Kitagawa, *Chem. Lett.*, 2015, **44**, 1694.
- 2 (a) L. E. Kreno, K. Leong, O. K. Farha, M. Allendorff, R. P. Van Duyne and J. T. Hupp, *Chem. Rev.*, 2012, **112**, 1105; (b) Y.-W. Li, J.-R. Li, L.-F. Wang, B.-Y. Zhou, Q. Chen and X.-H. Bu, *J. Mater. Chem. A*, 2013, **1**, 495; (c) Z. Dou, J. Yu, Y. Cui, Y. Yang, Z. Wang, D. Yang and G. Qian, *J. Am. Chem. Soc.*, 2014, **136**, 5527.
- 3 (a) N. Guillou, Q. Gao, P. M. Forster, J. S. Chang, M. Noguès, S. E. Park, G. Férey and A. K. Cheetham, *Angew. Chem., Int. Ed.*, 2001, **40**, 2831; (b) A. Proust, R. Thouvenot and P. Gouzerh, *Chem. Commun.*, 2008, 1837; (c) J. Lee, O. K. Farha, J. Roberts, K. A. Scheidt, S. T. Nguyen and J. T. Hupp, *Chem. Soc. Rev.*, 2009, **38**, 1450; (d) Z.-J. Liu, S. Yao, Z.-M. Zhang and E.-B. Wang, *RSC Adv.*, 2013, **3**, 20829; (e) R. Kawahara, K. Niinomi, J. N. Kondo, M. Hibino, N. Mizuno and S. Uchida, *Dalton Trans.*, 2016, **45**, 2805.
- 4 (a) N. Stock and S. Biswas, *Chem. Rev.*, 2012, **112**, 933; (b) D. Kim, X. Song, J. H. Yoon and M. S. Lah, *Cryst. Growth Des.*, 2012, **12**, 4186; (c) T. Liu, D. Luo, D. Xu, H. Zeng and Z. Lin, *Inorg. Chem. Commun.*, 2013, **29**, 110; (d) P.-Z. Li, X.-J. Wang, Y. Li, Q. Zhang, R. H. D. Tan, W. Q. Lim, R. Ganguly and Y. Zhao, *Microporous Mesoporous Mater.*, 2013, **176**, 194; (e) Y.-X. Sun and W.-Y. Sun, *Chin. Chem. Lett.*, 2014, **25**, 823.
- 5 (a) R.-Q. Zhong, R.-Q. Zou, M. Du, T. Yamada, G. Maruta, S. Takeda and Q. Xu, *Dalton Trans.*, 2008, 2346; (b) H. Wang, Y.-Y. Wang, G.-P. Yang, C.-J. Wang, G.-L. Wen, Q.-Z. Shi and S. R. Batten, *CrystEngComm*, 2008, **10**, 1583; (c) B. Zheng, J. Bai and Z. Zhang, *CrystEngComm*, 2010, **12**, 49; (d) J.-X. Yang, X. Zhang, J.-K. Cheng, J. Zhang and Y.-G. Yao, *Cryst. Growth Des.*, 2012, **12**, 333; (e) H.-N. Wang, G.-S. Yang, X.-L. Wang and Z.-M. Su, *Dalton Trans.*, 2013, **42**, 6294; (f) K. P. Rao, M. Higuchi, J. Duan and S. Kitagawa, *Cryst. Growth Des.*, 2013, **13**, 981; (g) C. Patzschke, C. M. Forsyth, S. R. Batten and A. L. Chaffee, *CrystEngComm*, 2014, **16**, 6296.
- 6 (a) S.-T. Wu, L.-S. Long, R.-B. Huang and L.-S. Zheng, *Cryst. Growth Des.*, 2007, **7**, 1746; (b) R.-G. Lin, L.-S. Long, R.-B. Huang and L.-S. Zheng, *Inorg. Chem. Commun.*, 2007, **10**, 1257; (c) Q. Chu, G.-X. Liu, T. Okamura, Y.-Q. Huang, W.-Y. Sun and N. Ueyama, *Polyhedron*, 2008, **27**, 812; (d) M. Kouno, Y. Miyashita, N. Yoshinari and T. Konno, *Chem. Lett.*, 2015, **44**, 1512.
- 7 T. Konno, A. Toyota and A. Igashira-Kamiyama, *J. Chin. Chem. Soc.*, 2009, **56**, 26.
- 8 K. Nakamoto, *Infrared and Raman Spectra of Inorganic and Coordination Compounds*, Wiley, Chichester, 5th edn, 1997.
- 9 A. L. Spek, *J. Appl. Crystallogr.*, 2003, **36**, 7.
- 10 S. Surinwong, N. Yoshinari, B. Yotnoi and T. Konno, *Chem. – Asian J.*, 2016, **11**, 486.
- 11 N. Yoshinari, K. Tatsumi, A. Igashira-Kamiyama and T. Konno, *Chem. – Eur. J.*, 2010, **16**, 14252.
- 12 K. S. W. Sing, D. H. Everett, R. A. W. Haul, L. Moscou, R. A. Pierotti, J. Rouquerol and T. Siemieniowska, *Pure Appl. Chem.*, 1985, **57**, 603.
- 13 H. Furukawa, F. Gándara, Y.-B. Zhang, J. Jiang, W. L. Queen, M. R. Hudson and O. M. Yaghi, *J. Am. Chem. Soc.*, 2014, **136**, 4369.
- 14 (a) J. Canivet, A. Fateeva, Y. Guo, B. Coasne and D. Farrusseng, *Chem. Soc. Rev.*, 2014, **43**, 5594; (b) N. C. Burtch, H. Jasuja and K. S. Walton, *Chem. Rev.*, 2014, **114**, 10575.
- 15 (a) A. Nalaparaju, X. S. Zhao and J. W. Jiang, *J. Phys. Chem. C*, 2010, **114**, 11542; (b) A. Kobayashi, A. Sugiyama, T. Ohba, Y. Suzuki, H.-C. Chang and M. Kato, *Chem. Lett.*, 2014, **43**, 1070; (c) J. J. Gutiérrez-Sevillano, S. Calero and R. Krishna, *J. Phys. Chem. C*, 2015, **119**, 3658.

